

# Structure and chemical composition of water-grown oxides of GaAs

Z. Liliental-Weber

*Lawrence Berkeley Laboratory, 1 Cyclotron Road, Berkeley, California 94720*

C. W. Wilmsen and K. M. Geib

*NSF ERC for Optoelectronic Computing Systems and Department of Electrical Engineering, Colorado State University, Fort Collins, Colorado 80523*

P. D. Kirchner, J. M. Baker, and J. M. Woodall

*IBM T. J. Watson Research Center, Yorktown Heights, New York 10598*

(Received 27 March 1989; accepted for publication 31 October 1989)

Previously it has been shown that the electronic surface properties of GaAs can be improved by photochemical treatment in water. If this photowashing technique is carried out with intense white light, oxides several hundred angstroms thick can be grown. This paper reports the structure and composition of this photowashed oxide and one grown by soaking in stagnant water in low light. The oxide was determined by TEM cross sections to be highly porous, but with thin continuous oxide layers both at the surface and at the oxide/GaAs interface. The oxide is composed of  $\text{Ga}_2\text{O}_3$  with a low concentration of  $\text{As}_2\text{O}_3$ . The layer is primarily a fine grain Ga oxide crystal with a structure which appears different from the common forms of  $\text{Ga}_2\text{O}_3$ .

## I. INTRODUCTION

The recent reports<sup>1-4</sup> on the unpinning of the GaAs surface by photowashing in deionized water have caused a renewed interest in the process of water oxidation since the photowashing process results in the rapid growth of an oxide layer whose thickness is a linear function of photowashing time.<sup>5,6</sup> The thickness has been reported to saturate at about 950 Å after 18 min of photowashing at room temperature under intense light. In addition to unpinning, photowashing can be used to selectively oxidized areas on a wafer and the technique should aid in understanding the photo-oxidation of other semiconductors.

Previously, Schwartz<sup>7</sup> reported growing a 850-Å-thick oxide layer by placing a GaAs wafer in room-temperature stagnant water for six days. He also grew oxide layers in boiling water.<sup>8</sup> X-ray diffraction and electron microprobe analysis indicated that these oxides were composed of  $\text{Ga}_2\text{O}_3 \cdot \text{H}_2\text{O}$ . The oxide growth rate was found to be a strong function of the doping concentration of the GaAs.

This paper reports on the structure and chemical composition of oxides grown by both the photowashing and stagnant water processes. Transmission electron microscopy (TEM) of thinned cross sections were used to investigate the physical structure, the crystallinity, and the composition of the oxide layers. X-ray photoelectron spectroscopy (XPS) was also used to investigate the oxide composition.

## II. EXPERIMENTAL TECHNIQUE

The oxides were grown on (100) bulk *n*-type GaAs doped with  $3 \times 10^{17} \text{ cm}^{-3}$  Si; these wafer specifications are the same as previously used in photoluminescence studies.<sup>5,6</sup> The GaAs was first etched for 30 s in a 1:8:500 mixture of  $\text{H}_2\text{SO}_4:\text{H}_2\text{O}_2:\text{H}_2\text{O}$ , and rinsed with deionized (DI) water. The wafer was then either placed on a spinner and photowashed for a specified length of time or placed in a beaker containing DI water. The stagnant water samples

were soaked for 48 h in room light. The photowashed samples were held ~3 in. from a 300-W tungsten halogen projector bulb for 2, 4, or 18 min with a stream of DI water covering the surface.

Some of the photowashed samples were immediately placed in a beaker of methanol to protect them from air exposure. These samples were transferred wet with methanol into a dry box connected to the XPS analysis chamber. No special handling was used with the XPS profile or TEM cross section samples. As a result these samples were exposed to air for a number of days.

TEM cross-sectional samples were prepared by cleaving along {011} planes into 1-mm-wide strips, gluing the oxide sides together to allow viewing in the microscope with the electron-beam parallel to [011]. Silver epoxy was used as the glue. To harden this epoxy, the samples were kept for 30 min in the oven at 90 °C. As a next step, the samples were mechanically polished on both sides of the strips to decrease their thickness to approximately 30 μm. The samples prepared in this way were then Ar-ion milled in a low-temperature stage starting with 5 keV and finishing with 2 keV to obtain perforations in the area close to the glue. The area in the vicinity of the perforation is transparent to electrons.

## III. EXPERIMENTAL RESULTS

### A. Structure

The TEM cross sections show that both types of water-grown oxides have a similar structure which consists of a highly porous layer sandwiched between thin continuous oxide layers located at the surface and at the GaAs interface as shown in Figs. 1 and 2. We had previously<sup>5</sup> predicted the porosity of the oxide layer based on the rapid growth of the photowashed oxide at room temperature and the preliminary composition measurements. It was reasoned that both Ga and As oxides were formed by the water but that the As oxide was continuously washed away leaving a labyrinth of

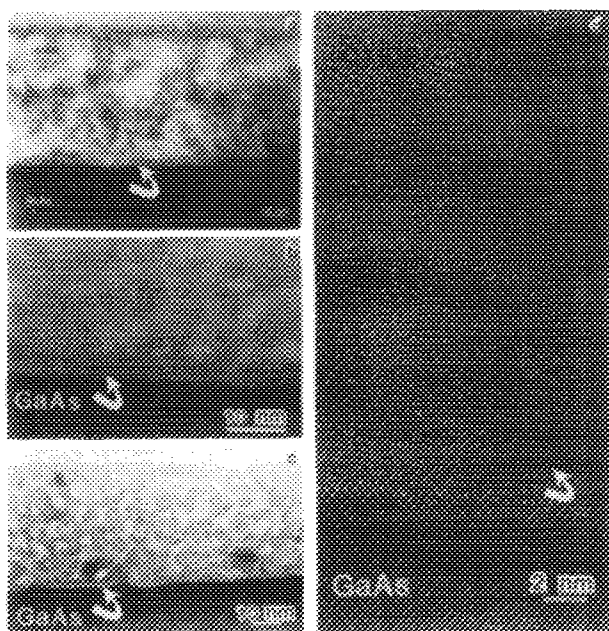


FIG. 1. TEM cross section of the GaAs sample formed by photowashing for 18 min; (a) and (c) whole layer; note lack of pores at the interface (marked by arrow) and at the top of the layer, flat top surface, and pores in the middle part of the layer; (b) higher magnification of area of interface with continuous layer; and (d) lattice image of pore area showing crystalline particles arranged in random orientation.

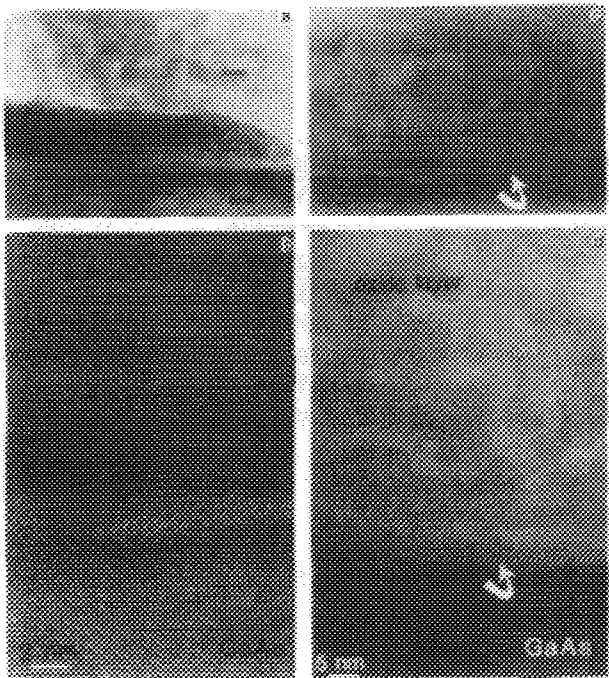


FIG. 2. TEM cross section of the GaAs sample formed by photowashing for 48 h in DI stagnant water: (a) elongated monocrystalline particle with twins at the GaAs interface; (b) round twinned monocrystalline particle at the GaAs interface; (c) entire layer showing the formation of larger monocrystalline particles in the area close to the interface, the formation of a continuous layer at the interface, pores in the middle of the layer, and a more undulating surface compared to the previous sample; and (d) high-resolution micrograph of the interfacial area showing a continuous layer and polycrystalline grains with pores above this layer.

$\text{Ga}_2\text{O}_3$ . Since this porous structure allowed water to reach the GaAs surface, thick oxide layers could be grown. The TEM results presented support this model.

The pore structure of oxides grown by the two methods was found to be similar, however the pores in the stagnant water-grown oxide are approximately twice as large as the pores in the photowashed oxide. In the photowashed oxide, the pore size increases from  $\sim 3$  nm near the interface to  $\sim 8$  nm near the oxide surface. In the stagnant water oxide the pore size ranges up to  $\sim 15$  nm.

High-resolution images from the porous area [Figs. 1(d) and 2(b)] show that the oxide is composed of randomly oriented fine grains. The micrographs also show that the GaAs surface appears to have been roughened by the water oxidation, although no control sample was used to verify this observation. The stagnant water sample has the rougher oxide/GaAs interface. The oxide grown in stagnant water has another salient feature, the presence of large monocrystalline particles (spherical or elongated, 5–100 nm in size) in the areas near the interface [Figs. 2(a)–2(c)]. In the areas where large crystalline particles formed, the interface is more undulated.

This porous layer is sandwiched between two thin continuous oxide layers ( $\approx 4$  nm thick at the interface and  $\approx 6$  nm at the surface). The origin of these layers is not clear, although the long air exposure required to form the cross sections for TEM analysis is expected to grow some oxide since  $\text{O}_2$  can pass through the pores where it could react with the GaAs substrate.

## B. Chemical composition

Several different types of analysis were used to determine the chemical composition of the water-grown oxides. All of the techniques showed that the composition of the oxides grown by photowashing and stagnant water are quite similar. In all cases the Ga/As ratio  $\geq 1$ . This section discusses the results of each of the techniques.

### 1. X-ray photoelectron spectroscopy (XPS)

Two types of XPS tests were performed. The first examined just the surface of oxides grown with different photowash times, 2, 4, and 18 min. Since the oxide thickness is a function the photowashing time, a rough profile of the oxide layer is obtained by this method. The samples were immediately placed in methanol after the photowashing and transferred within 5 min, wet with methanol, into an oxygen-free dry box connected to the XPS chamber. Thus, the samples were exposed directly to air for only a few seconds after oxide growth. Previous tests showed that the methanol gave good protection against oxidation.

The Ga and As  $3d$  lines for these three samples are illustrated in Fig. 3. Table I lists the important parameters obtained from these data. The Ga/As ratio is seen to range from 8 to 16, thus, the oxide is highly Ga rich. The difference in binding energy  $\Delta\text{BE}$  between the arsenic oxide and the GaAs substrate is  $\approx 3.7$  eV which corresponds<sup>9,10</sup> to the +3 oxidation state for the As. No peak is observed at  $\Delta\text{BE} = 5.0$  and thus no As in the +5 oxidation state is observed. This

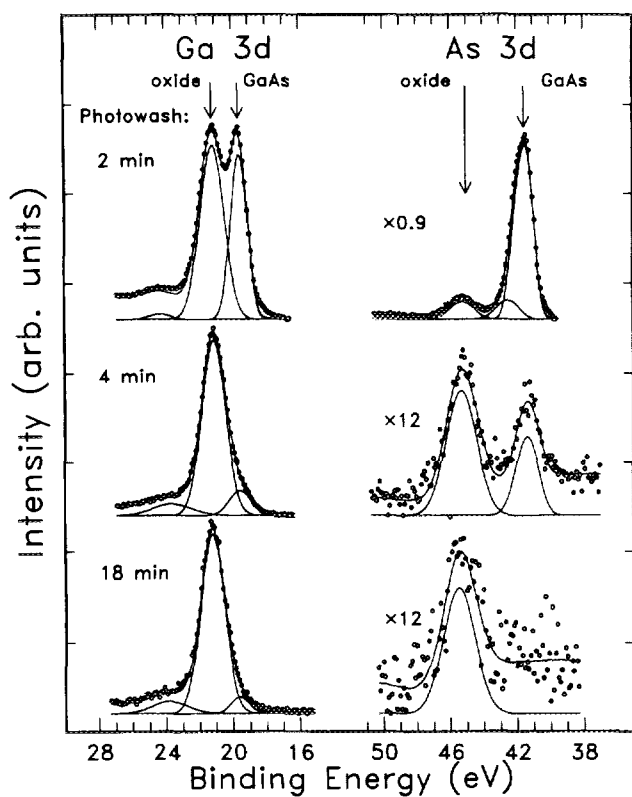


FIG. 3. XPS analysis of the surface of photowashed oxides grown for 2, 4, and 18 min. The Ga and As $3d$  lines are shown.

means that the arsenic oxide on the surface of the photowashed layer is in the form  $\text{As}_2\text{O}_3$  and not  $\text{As}_2\text{O}_5$  or  $\text{GaAsO}_4$ . The Ga oxide—GaAs  $\Delta\text{BE}$  is observed to be  $\approx 1.6$ , which is close to the  $1.4 \pm 0.2$  eV reported<sup>9,10</sup> for  $\text{Ga}_2\text{O}_3$  and  $\text{GaAsO}_4$ . Thus, the XPS indicates that the photowash oxide is primarily a form of  $\text{Ga}_2\text{O}_3$  (possibly hydrated) with a small component of  $\text{As}_2\text{O}_3$ .

XPS sputter profiling was performed on 600- to 900-Å-thick oxides grown by both the stagnant water and the photowashing techniques as shown in Fig. 4. These samples were exposed to air for several days and thus some changes may have occurred from the “as grown” condition. Both of the profiles indicate Ga/As ratio of  $> 8$  which is nearly constant throughout the layer. The surface is seen to contain only Ga and As oxides but the sputter beam rapidly decomposes some of the arsenic oxide into elemental As.

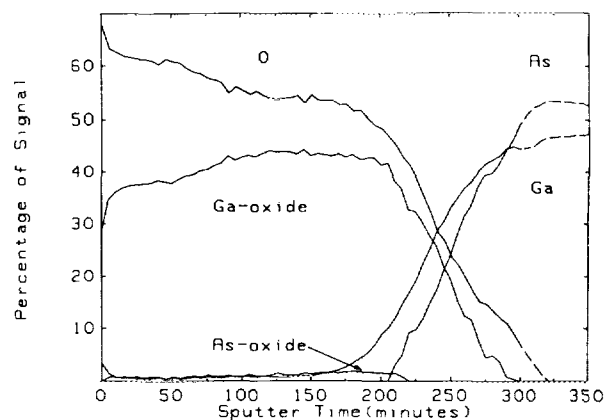
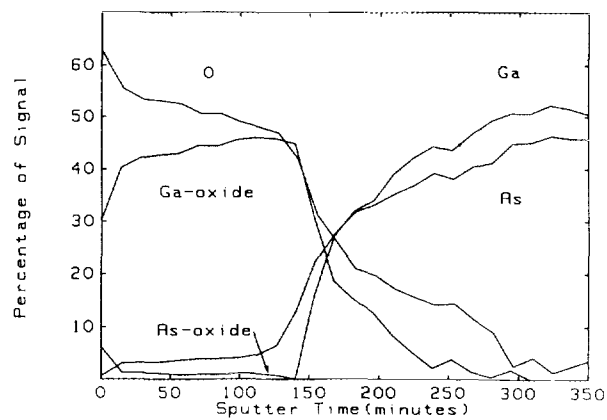


FIG. 4. XPS profiles of (a) photowashed oxide and (b) stagnant water-grown oxide.

The Ga-As-O ratios were obtained by measuring the areas of XPS peaks and dividing by the sensitivity factors, which for our XPS system are: O—0.63, Ga—0.30, and As—0.33. As a result, the photowashed oxide has a normalized ratio of 1.0/0.12/1.3 and the stagnant water oxide has a ratio of 1.0/0.04/1.5. If the oxide layer is composed of a mixture of  $\text{Ga}_2\text{O}_3$  and  $\text{As}_2\text{O}_3$ , then the ratio would be 1.0/ $X$ /1.5, where  $X$  is the  $\text{As}_2\text{O}_3/\text{Ga}_2\text{O}_3$  mixture ratio. Therefore, the measured Ga-As-O ratios suggest that the oxide layer is indeed a mixture of  $\text{Ga}_2\text{O}_3$  and  $\text{As}_2\text{O}_3$ .

TABLE I. Binding energies of the Ga $3d$  and As $3d$  XPS lines observed at the surface of oxides photowashed for 2, 4, and 18 min.

Photowash Time	Ga $3d$			As $3d$			
	Substrate (eV)	Oxide (eV)	$\Delta\text{BE}$ (eV)	Substrate	Oxide	$\Delta\text{BE}$	Ga-O/As-O
2 min	18.7	20.3	1.6	40.7	44.4	3.7	8
4	...	20.4	...	40.6	44.4	3.8	16
18	...	20.2	...	...	44.4	...	14

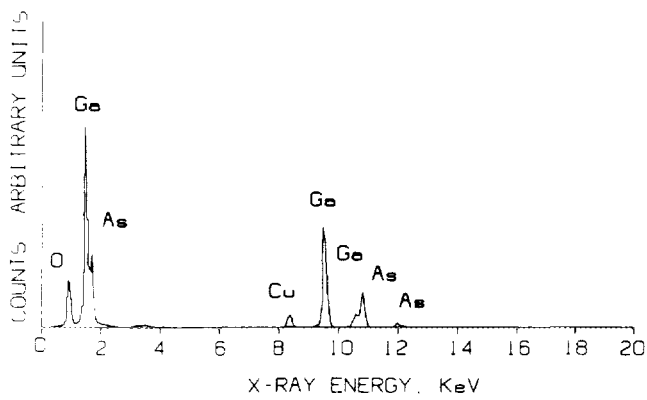


FIG. 5. EDX spectrum from the sample kept for 48 h in stagnant DI water.

## 2. Electron diffraction, energy dispersive x-ray, and other techniques

A number of techniques using the electron beam of the TEM were applied in order to corroborate and extend the XPS results. These data provide additional insight into the composition and structure of the water-grown oxides.

Energy dispersing x rays (EDX) from a 30-nm-diam electron beam were used to determine the Ga-As-O ratio of the oxide layer (Fig. 5). This measurement indicated a ratio of 1.0/0.4/1.6. In agreement with the XPS results, this ratio indicates that on the average the oxide is composed of a mixture of  $\text{Ga}_2\text{O}_3$  and  $\text{As}_2\text{O}_3$ . However, the concentration of As measured by EDX is much higher than that obtained from XPS which may be the result of reflections from the GaAs substrate.

In addition, selected area diffraction (SAD) patterns were obtained from the porous regions with the electron beam overlapping the continuous oxide layers and the GaAs substrate. The SAD patterns form typical rings [Figs. 6(a) and 6(e)] which correspond to the GaAs and to 2.4-, 2.0-, and 1.45-Å interplanar spacings of the oxide layer. These spacings are corroborated by high resolution images of the porous area which show randomly oriented grains with interplane spacings of 2.4 and 2.0 Å [Fig. 1(d)].

These lattice spacings are not simply explained, however, since none of the Ga or As oxides listed in the ASTM diffraction file data correspond exactly.<sup>11</sup> The various forms of  $\text{Ga}_2\text{O}_3$  ( $\alpha$ ,  $\beta$ ,  $\delta$ ,  $\epsilon$ , and  $\gamma$ ) all have strong diffraction intensities at the 2.4-, 2.0-, and 1.45-Å spacing. Unfortunately, the ASTM data files also indicate strong intensities at a number of other spacings for these crystalline phases. The  $\gamma$  phase has the fewest diffracting planes. However,  $\gamma$ - $\text{Ga}_2\text{O}_3$  is cubic with the 2.4-Å spacing associated with the (113) plane and the 2.0 Å with the (004) plane. While the angle between these two cubic planes should be 25°, the angle measured on the micrographs is 70° which fits a fcc or diamond lattice. Since both the XPS and EDX clearly show that the layer is primarily composed of a Ga oxide, we conclude that a new crystalline form of  $\text{Ga}_2\text{O}_3$  is grown by the water. The oxide may contain some water.

In order to extract additional information from the continuous layer near the interface, laser diffraction patterns from the high-resolution micrographs were obtained. These gave the same three lattice spacings as discussed above. In addition, extra spots corresponding to a 4.79 Å lattice spacing are also observed [Figs. 6(c), 6(d), and 6(f)–6(h)]. The 4.79-Å spots also appeared in some of the diffraction patterns of the continuous layer at the surface. This lattice spac-

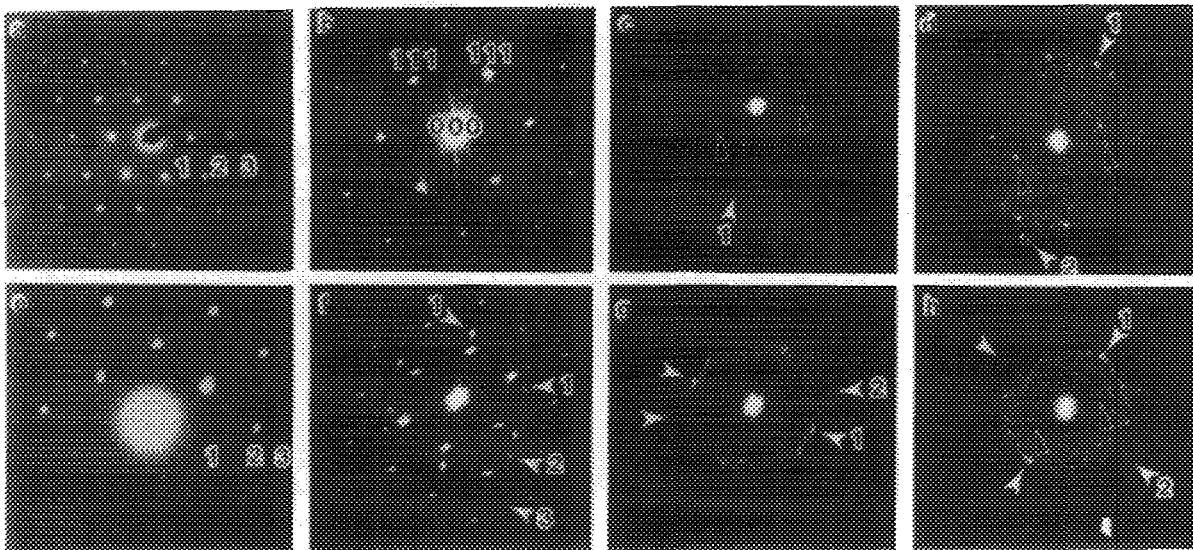


FIG. 6. SAD patterns and laser diffraction patterns from GaAs samples photowashed for 18 min (a)–(d) and photowashed for 48 h in stagnant DI water (e)–(h). Interplanar distances at 2.4 Å are marked by 1, at 2.0 Å by 2, and at 1.45 Å by 3. Extra spots at 4.79 Å are marked by black arrows. (a) SAD diffraction pattern showing double diffraction from monocrystalline GaAs (dot pattern) and polycrystalline ring pattern from the layer; (b) laser diffraction pattern from the GaAs; (c) from the continuous layer area close to the interface; (d) from the area close to the top of the layer; (e) SAD diffraction pattern from the sample kept for 48 h in DI stagnant water—note the same arrangement of the diffraction spots from the substrate and the ring pattern from the layer as in the previous sample; (f) laser diffraction pattern from the interface between GaAs and large crystalline particle shown in Fig. 3(b); (g) from the area close to the interface; and (h) from the top of the layer.

ing does not correspond to any of the  $\text{Ga}_2\text{O}_3$  spacings except the  $\beta$  form which has a 60% intensity at 4.65 Å. The  $\alpha$  form of GaOH also has strong intensities at all four of the spacings but it too has strong intensities from many other planes. Therefore it appears that the 4.79-Å spot is associated with an As oxide. The  $\text{As}_2\text{O}_5$  has its maximum intensity at 4.88 Å with no other strong peaks. However, the XPS results shown in Fig. 4(b) clearly show that  $\text{As}_2\text{O}_5$  is not present. In addition  $\text{As}_2\text{O}_5$  is highly soluble. Therefore, it is doubtful that  $\text{As}_2\text{O}_5$  is present in the oxide layers.

#### IV. CONCLUSIONS

The TEM cross sections clearly show that the water-grown oxides are porous with pore sizes ranging from 3 to 15 nm. These pores apparently form by the selective dissolution of the arsenic oxide. As a result, the oxide layers are primarily composed of  $\text{Ga}_2\text{O}_3$ , however, some arsenic oxide remains in the layer. The  $\text{Ga}_2\text{O}_3$  appears to be in the form of fine grain crystallites. The diffraction patterns indicate that the crystalline form has been altered from the known phases of  $\text{Ga}_2\text{O}_3$ , which may be hydrated as suggested by Schwartz.<sup>7</sup>

The TEM cross sections also show that the porous layer is sandwiched between two thin continuous oxide layers. It is not known at present if these layers form during water growth or subsequently as a result of air exposure. There are indications that these continuous layers have a higher con-

centration of As oxide. This As oxide may influence the surface pinning, but further work is required.

#### ACKNOWLEDGMENTS

The work was supported by the Materials Science Division of the U.S. Department of Energy under Contract No. DE-AC03-76SF00098 and by the National Science Foundation Grant No. CDR 8622236. The use of the electron microscopy facility at the National Center for Electron Microscopy at LBL in Berkeley, CA is greatly appreciated.

<sup>1</sup>S. D. Offsey, J. M. Woodall, A. C. Warren, P. D. Kirchner, T. I. Chappell, and G. D. Pettit, *Appl. Phys. Lett.* **48**, 475 (1986).

<sup>2</sup>S. M. Beck and J. E. Wessel, *Appl. Phys. Lett.* **50**, 149 (1987).

<sup>3</sup>N. A. Ives, G. W. Stupian, and M. S. Leung, *Appl. Phys. Lett.* **50**, 256 (1987).

<sup>4</sup>P. D. Kirchner, A. C. Warren, J. M. Woodall, C. W. Wilmsen, S. L. Wright, and J. M. Baker, *J. Electrochem. Soc.* **135**, 1822 (1988).

<sup>5</sup>C. W. Wilmsen, P. D. Kirchner, J. M. Baker, D. T. McInturff, G. D. Pettit, and J. M. Woodall, *J. Vac. Sci. Technol. B* **6**, 1180 (1988).

<sup>6</sup>C. W. Wilmsen, P. D. Kirchner, and J. M. Woodall, *J. Appl. Phys.* **64**, 3287 (1988).

<sup>7</sup>B. Schwartz, *J. Electrochem. Soc.* **118**, 657 (1971).

<sup>8</sup>B. Schwartz, S. E. Haszlev, and D. R. Wonsidler, *J. Electrochem. Soc.* **118**, 1229 (1979).

<sup>9</sup>Y. Mizokawa, H. Iwasaki, R. Nishitani, and S. Nakamura, *J. Electron Spectrosc. Relat. Phenom.* **14**, 129 (1978).

<sup>10</sup>G. P. Schwartz, G. J. Gualtieri, G. W. Kammlott, and B. Schwartz, *J. Electrochem. Soc.* **126**, 1737 (1979).

<sup>11</sup>A. S. T. M. Powder diffraction data files, 1984.